Available online at www.sciencedirect.com
SCIENCE DIRECT
ELSEVIER
Icarus 172 (2004) 170–178
ICARUS
www.elsevier.com/locate/icarus

Radar detection of near-Earth Asteroids 1915 Quetzalcoatl, 3199 Nefertiti, 3757 (1982 XB), and 4034 (1986 PA)

Michael K. Shepard [a,*], Lance A.M. Benner [b], Steven J. Ostro [b], Donald B. Campbell [c], Irwin I. Shapiro [d], John F. Chandler [d]

[a] *Department of Geography and Geosciences, Bloomsburg University, Bloomsburg, PA 17815, USA*
[b] *Jet Propulsion Laboratory, Pasadena, CA 91109, USA*
[c] *National Astronomy and Ionosphere Center, Cornell University, Ithaca, NY 14853, USA*
[d] *Harvard-Smithsonian Center for Astrophysics, Cambridge, MA 02138, USA*

Received 10 March 2004; revised 2 June 2004

Available online 28 July 2004

Abstract

We describe Arecibo (2380 MHz, 12.6 cm) Doppler-only radar detections of near-Earth Asteroids 1915 Quetzalcoatl, 3199 Nefertiti, 3757 (1982 XB), and 4034 (1986 PA) obtained between 1981 and 1989. Estimates of the echo spectral bandwidths, radar cross-sections, and circular polarization ratios of these objects constrain their sizes, radar albedos, surface roughnesses, taxonomic classes, rotation periods, and pole directions. Our radar constraints on the diameters of Quetzalcoatl and Nefertiti are most consistent with sizes determined using thermal-radiometry and the Fast Rotation Model (FRM); this consistency may indicate that these asteroids have surfaces of high thermal inertia (i.e., little or no regolith). Constraints on Quetzalcoatl's radar albedo rule out a "metallic M" classification. The radar constraints for Nefertiti are inconsistent with a rotation pole published by Kaasalainen et al. (2004, Icarus 167, 178). Our estimates of 1982 XB's size are consistent with previously published estimates. The radar bandwidth of 1986 PA places an upper bound of about 24 h on its rotation period.
© 2004 Elsevier Inc. All rights reserved.

Keywords: Asteroids; Radar

1. Introduction

We report analyses of the first radar observations of near-Earth Asteroids (NEAs) 1915 Quetzalcoatl, 3199 Nefertiti, 3757 (1982 XB), and 4034 (1986 PA), from observations conducted at Arecibo between 1981 and 1989. Our observations achieved signal-to-noise ratios (SNRs) sufficient to place constraints on each target's physical characteristics. Preliminary results for all four objects were published by Ostro et al. (1991a); in this paper we expand upon those results and incorporate ancillary lightcurves, absolute magnitudes, and infrared radiometry into our analyses. Rotation period estimates exist for Quetzalcoatl, Nefertiti, and 1982 XB, but not for 1986 PA. Table 1 provides a summary of our targets' previously reported physical properties.

2. Observations

Our observational, reduction, and analysis techniques are similar to those described by Mitchell et al. (1995) and Ostro et al. (2002). Table 2 summarizes key observational parameters. Each observing run consisted of transmission of a circularly polarized, 2380 MHz (12.6 cm) continuous-wave (cw) signal for the round-trip light travel time to the target, followed by reception of echoes for a comparable duration in the opposite (OC) and same (SC) senses of polarization as transmitted. When Quetzalcoatl was observed in 1981, the Arecibo receiver was able to receive only one polarization at a time and alternating runs were switched between OC and SC echoes. OC and SC echoes were received simultane-

* Corresponding author. Fax: 570-389-3028.
E-mail address: mshepard@bloomu.edu (M.K. Shepard).

0019-1035/$ – see front matter © 2004 Elsevier Inc. All rights reserved.
doi:10.1016/j.icarus.2004.06.003

Table 1
Physical properties

Asteroid	a (AU)	e	i (°)	H	p_v	D (km)	Class	P (h)	Δm
1915 Quetzalcoatl	2.54	0.572	20.4	18.97[a]	0.16–0.42[b,c]	0.3–0.56[b,c]	SMU[d,e]	4.9 ± 0.3[d]	0.2[d]
3199 Nefertiti	1.57	0.284	33.0	15.13[f]	0.26–0.41[b]	1.8–2.2[b]	S[e], A[g], Sq[h]	3.0207[f]	0.11–0.30[f]
3757 1982 XB	1.83	0.446	3.9	19.12[i]	0.09–0.26[b,i,j]	0.35–0.7[b,i,j]	S[e]	9.0046[j]	0.14[j]
4034 1986 PA	1.06	0.444	11.2	18.10[k]	0.29–0.58[l]	0.40–0.57[l]	O[m]	–	–

Notes. a, e, and i are the semimajor axis, eccentricity, and inclination of the asteroid's orbit. H is the asteroid's absolute magnitude. p_v is the range of reported optical geometric albedos. D is the range of reported effective diameters in kilometers. Class refers to taxonomic class (Tholen and Barucci, 1989; Bus and Binzel, 2002). P is the synodic rotation period in hours. Δm is the visual lightcurve amplitude in magnitudes. The taxonomic classes and values of H, p_v, D, P, and Δm were taken from the references indicated.

[a] Rabinowitz et al. (1994). [b] Veeder et al. (1989). [c] Harris and Lagerros (2002). [d] Binzel and Tholen (1983). [e] Tholen (1989). [f] Pravec et al. (1997). [g] Cruikshank et al. (1985). [h] Bus and Binzel (2002). [i] Helin et al. (1983). [j] Harris et al. (1999). [k] http://ssd.jpl.nasa.gov/horizons.html. [l] Delbo et al. (2003). [m] Binzel et al. (2004).

Table 2
Observations

Target	Dates (UTC)	RA (°)	DEC (°)	Runs	Δt (UTCh)	$\Delta\phi$ (°)	Distance (AU)	Res'n (Hz)	Sky motion (°)
1915 Quetzalcoatl	1981 Mar 5	163.4	13.2	22	03:18–05:44	0–180	0.087	1.2	
	1981 Mar 6	167.6	16.8	22	03:33–05:54	342–154	0.089	1.2	
	1981 Mar 7	170.7	20.2	21	03:44–06:04	319–130	0.092	1.2	21
	1981 Mar 8	173.6	23.2	11	03:51–05:07	290–23	0.096	1.2	
	1981 Mar 9	176.6	26.1	19	04:02–06:15	267–70	0.100	1.2	
	1981 Mar 10	179.3	28.6	13	04:36–06:10	272–27	0.105	1.2	
3199 Nefertiti	1986 Sep 5	352.0	17.4	16	03:40–06:02	0–279	0.222	0.5	
	1986 Sep 6	350.4	19.6	16	03:36–05:00	332–256	0.221	0.5	
	1986 Sep 7	348.8	21.8	19	03:22–05:46	285–211	0.221	0.5	11
	1986 Sep 8	347.1	23.9	16	03:39–05:40	299–176	0.220	0.5	
	1986 Sep 9	345.4	26.1	16	03:08–05:21	218–122	0.221	0.5	
3757 (1982 XB)	1987 Dec 2	129.0	17.9	36	06:51–09:09	350–82	0.077	1.0	
	1987 Dec 3	132.2	18.1	34	07:06–09:18	239–327	0.078	1.0	
	1987 Dec 5	135.5	18.3	45	07:10–09:46	0–104	0.079	0.1	9
	1987 Dec 6	138.4	18.4	39	07:25–09:55	250–350	0.080	0.1	
4034 (1986 PA)	1989 Mar 24	330.2	21.5	7	14:03–15:33	–	0.162	0.12	
	1989 Mar 25	328.0	23.0	8	13:57–14:47	–	0.160	0.12	8
	1989 Mar 26	325.7	24.5	25	12:39–15:11	–	0.158	0.12	
	1989 Mar 27	323.3	25.9	18	13:04–14:56	–	0.156	0.12	

Notes: Runs refers to the number of transmit-receive cycles. For Quetzalcoatl, OC and SC are separate runs; for the remaining asteroids, each run is dual-polarization. Δt refers to the start and stop receive-time. $\Delta\phi$ is the rotation phase of the target using the end of the first run as 0° phase. Epochs for 0° relative rotation phase: Quetzalcoatl, 1981 March 5, 03:17:54 UTC; Nefertiti, 1986 September 5, 03:43:41 UTC; 1986 XB, 1987 December 5, 07:11:20 UTC. Sky motion refers to the total change in apparent position between the first and last observation for each target. For all asteroids, the minimum system temperature was between 33 and 42 K; maximum system gain was 71 dB.

ously for Nefertiti, 1982 XB, and 1986 PA. Our reduction of raw echo power spectra included background removal, calibration, and the formation of sums of spectra weighted by signal strength.

The radar albedo, $\hat{\sigma}_{\rm OC}$, of an asteroid is the ratio of its OC radar cross-section ($\sigma_{\rm OC}$) to its cross-sectional area,

$$\hat{\sigma}_{\rm OC} = \frac{4\sigma_{\rm OC}}{\pi D_{\rm eff}^2}, \tag{1}$$

where the effective diameter $D_{\rm eff}$ is the diameter of a sphere with the same projected area as the target. Thus, $\hat{\sigma}_{\rm OC}$ can vary with aspect for targets with aspherical shapes or non-uniform reflection properties. Published asteroid radar albedos vary from a low of 0.04 for the G-class Main-Belt Asteroid (MBA) 1 Ceres (Mitchell et al., 1996) and NEA 1566 Icarus (Mahapatra et al., 1999) to a maximum of 0.58 for the M-class NEA 6178 (1986 DA) (Ostro et al., 1991b). For a summary of asteroid radar properties, see http://echo.jpl.nasa.gov/~lance/asteroid_radar_properties.html.

The instantaneous bandwidth B of a radar echo is related to the radar wavelength λ, the target's physical properties, and its orientation by

$$B(\phi) = \frac{4\pi D(\phi)}{\lambda P}\cos\delta, \tag{2}$$

where $D(\phi)$ is the asteroid's plane-of-sky extent normal to the apparent spin vector at rotation phase ϕ, P is the apparent rotation period, and δ is the angle between the radar line-of-sight and the object's apparent equator. With D in km, B in Hz, P in h, and λ of 12.6 cm, Eq. (2) can be rewrit-

ten

$$D(\phi) = \frac{PB(\phi)}{27.7\cos\delta}. \quad (3)$$

For each target we estimate the minimum bandwidth and the corresponding lower bound on the maximum pole-on breadth, $D_{\max}$, using Eq. (3). For moderate SNR targets (Nefertiti and 1982 XB), our experience with other asteroids suggests that a reasonable estimate of the bandwidth can be made from the points where the echo power spectrum first drops to two standard deviations of the background noise (referred to as two-sigma crossing thresholds). For low SNR targets (Quetzalcoatl and 1986 PA) we use more conservative estimates as noted for each. Uncertainties in our estimates of radar cross-section (obtained by integrating the spectra) are ±35% (±50% for Quetzalcoatl) and are based on prior experience with systematic uncertainties in pointing and calibration. Because systematic uncertainties are nearly the same for both polarization senses, our uncertainties in polarization ratio (ratio of SC to OC radar cross-section) are due primarily to receiver noise. Unless otherwise stated, our quoted uncertainties for random errors are one-standard deviation.

To place additional constraints on a target's diameter, we use the empirical relationship between optical albedo (p_v), effective diameter (D_{eff}, in km) and absolute magnitude (H) given by Fowler and Chillemi (1992):

$$\log p_v = 6.247 - 2\log D_{\text{eff}} - 0.4H. \quad (4)$$

We compare radar-derived diameter estimates with those derived from infrared radiometry using up to three different thermal models. The standard thermal model (STM) assumes a non-rotating spherical target with a low surface thermal inertia (i.e., a thick regolith). Lebofsky et al. (1978) developed the fast rotation model (FRM) because STM optical albedo estimates for several near-Earth asteroids were found to be significantly higher than expected from their spectral classification (see also Veeder et al., 1989). The FRM differs from the STM in that it assumes rapid rotation and/or a surface of high thermal inertia (i.e., rocky with no substantial regolith; see Lebofsky and Spencer, 1989). More recently, the Near-Earth Asteroid Thermal Model (NEATM) was developed by Harris (1998) to deal with the higher phase angles commonly observed in the NEA population and to allow more flexibility with certain model parameters (Harris and Lagerros, 2002).

3. Results

3.1. 1915 Quetzalcoatl

1915 Quetzalcoatl was classified as SMU by Tholen (1989). The U is not a separate class, but an appendage that indicates an unusual spectrum (Tholen and Barucci, 1989). Radiometrically determined estimates of Quetzalcoatl's diameter are 0.3 km (Veeder et al., 1989) and 0.34 km (Harris and Lagerros, 2002) using the STM, 0.4 km using the NEATM (Harris and Lagerros, 2002) and 0.5 km (Veeder et al., 1989) and 0.56 km (Harris and Lagerros, 2002) using the FRM. A synodic rotation period of 4.9 ± 0.3 h was reported by Binzel and Tholen (1983).

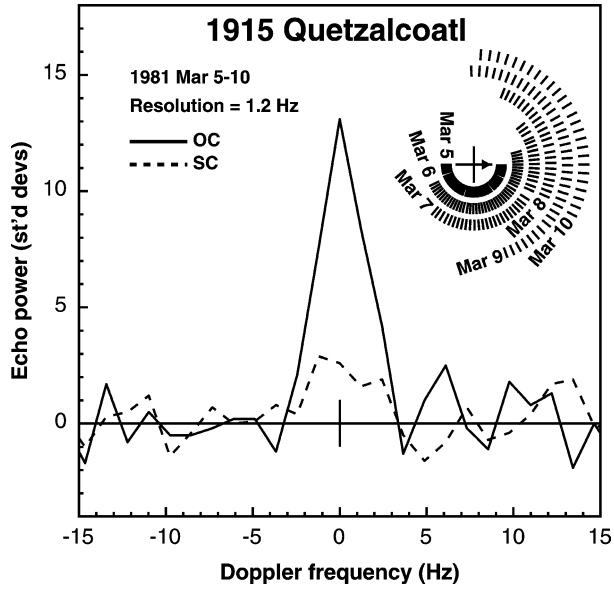

Fig. 1. Weighted sum of 1915 Quetzalcoatl echo power spectra. Frequency resolution is 1.2 Hz. A vertical bar at the origin indicates ±1 standard deviation of the OC receiver noise. Relative rotation phases for each date (one bar per run) are plotted in the upper right corner beginning at 0° for UTC epoch 1981 March 5 03:17:54.

We analyzed 217 alternating OC and SC runs from March 5–10, 1981. Figure 1 shows a weighted sum of all OC runs, which have a total SNR of about 13. The following analysis is based on this weighted sum.

Quetzalcoatl's polarization ratio, $\mu_c = 0.27 \pm 0.08$, is about average for reported NEAs (Ostro et al., 2002; http://echo.jpl.nasa.gov/~lance/asteroid_radar_properties.html). Its radar cross-section is $\sigma_{\text{OC}} = 0.02 \pm 0.01$ km^2 (Table 3). Because of the relatively coarse frequency resolution and low SNR, we conservatively estimate Quetzalcoatl's bandwidth to be at least $B = 3.6$ Hz which is based on observing three frequency bins (1.2 Hz each) with an SNR > 3. Given a rotation period of 4.9 h, this bandwidth corresponds to a lower bound on Quetzalcoatl's maximum diameter $D_{\max}$ of 0.6 km (Table 4). If the optical albedo of an SMU-class asteroid is at least 0.10 (see Tholen and Barucci, 1989; Harris and Lagerros, 2002), then using Eq. (4) and Quetzalcoatl's absolute magnitude (Table 1) lead to an effective diameter of less than 0.7 km.

The radar data were insufficient to constrain Quetzalcoatl's aspect ratio (ratio of maximum to minimum diameter). However, its lightcurve amplitude (Table 1) suggests a modest aspect ratio of 1.2. Using our constraint on $D_{\max}$ and modeling Quetzalcoatl as an ellipsoid of aspect ratio $a/b = a/c = 1.2$ gives a D_{eff} of at least 0.5 km. Using this value as a lower bound, we place upper limits of 0.18 on Quetzalcoatl's optical albedo and 0.10 on its radar albedo.

Table 3
Radar properties

Asteroid	OC SNR	B (Hz)	σ_{OC} (km^2)	μ_c
1915 Quetzalcoatl	13	3.6	0.02 ± 0.01	0.27 ± 0.08
3199 Nefertiti	38	25.5	1.2 ± 0.4	0.47 ± 0.04
3757 (1982 XB)	39	1.4	0.017 ± 0.006	0.24 ± 0.05
1987 Dec 2, 3	23	–	0.015 ± 0.005	0.21 ± 0.04
1987 Dec 5, 6	31	1.4	0.018 ± 0.006	0.27 ± 0.05
4034 (1986 PA)	7	0.5	0.021 ± 0.007	0.21 ± 0.06

Notes: OC SNR is the optimally filtered SNR for the OC echo, B is the minimum bandwidth for each target (see text for details). σ_{OC} is the radar cross-section. μ_c is the polarization ratio. The entry for 1982 XB lists the weighted average for the total experiment and for dates of the same frequency resolution: Dec 2 and 3 (1 Hz), Dec 5 and 6 (0.1 Hz). The uncertainties listed for the average are conservative and based on the larger of those listed for the daily pairs.

Table 4
Radar constraints on physical properties

Target	D_{max} (km)	D_{eff} (km)	$\hat{\sigma}_{OC}$	p_v	Aspect ratio	Subradar latitude (°)
1915 Quetzalcoatl	$\geqslant 0.60$	0.5–1.0	$\leqslant 0.10$	$\leqslant 0.18$		
3199 Nefertiti	$\geqslant 2.8$	2.2–4.0	$\leqslant 0.32$	$\leqslant 0.20$	$\leqslant 1.5$	$\leqslant 55$
3757 (1982 XB)	$\geqslant 0.46$	0.4–0.6	$\leqslant 0.14$	$\leqslant 0.25$	$\leqslant 1.2$	$\leqslant 50$
4034 (1986 PA)	–	0.42*	0.15	–		

D_{max} is the maximum diameter of the pole-on silhouette (see text). D_{eff} is the probable range of effective diameters based on incorporation of ancillary data (optical or radar albedo information, see text for discussion), and $*$ indicates D_{eff} assumed based on infrared radiometry (Delbo et al., 2003). $\hat{\sigma}_{OC}$ is the upper bound on the radar albedo based on smallest D_{eff} indicated. p_v is the upper bound on the optical albedo based on smallest D_{eff} indicated. Aspect ratio is (maximum diameter)/(minimum diameter) indicated by rotational bandwidth variations. Subradar latitude is the angle between radar line-of-sight and the asteroid's equator.

If we assume a lower limit of 0.04 for Quetzalcoatl's radar albedo (based on the lowest radar albedo observed on any asteroid to date), then its effective diameter can be no larger than 1.0 km. Our size constraints are most consistent with radiometric thermal models that assume considerable surface thermal inertia, suggesting that Quetzalcoatl may lack a regolith.

Our radar albedo constraint is consistent with an S classification. Based on radar observations, Margot and Brown (2003), Ostro et al. (2000), Magri et al. (1999), and Ostro et al. (1991b) have observed that some M-class asteroids appear to be more metallic (radar albedo greater than ~ 0.3) while others appear to be more stony (radar albedo less than ~ 0.3). Our radar albedo constraint is inconsistent with a dominantly metallic composition, but may still permit Quetzalcoatl to be a non-metallic M-class object.

3.2. 3199 Nefertiti

3199 Nefertiti has been proposed as a possible source of pallasite meteorites based on its spectral similarity to mixtures of olivine and metal (Cruikshank et al., 1985). It has been classified as A, S, and Sq-class (Cruikshank et al., 1985; Tholen, 1989; Bus and Binzel, 2002, respectively). Estimates of Nefertiti's size from infrared radiometry range from 1.8 km (STM) to 2.2 km (FRM) (Veeder et al., 1989). Its synodic rotational period is $P = 3.0207 \pm 0.0002$ h (Pravec et al., 1997). Using lightcurves from five encounters between 1996 and 2003, Kaasalainen et al. (2004) present a shape model with aspect ratios $a/b = 1.1$ and $a/c = 1.2$, and report a pole direction of $\lambda = 197°$, $\beta = -22°$, with an uncertainty of 5°–10°.

Nefertiti was observed at Arecibo on September 5–9, 1986. A total of 83 dual-polarization runs were acquired with a total OC SNR of about 38. Figure 2 shows a weighted sum of each day's runs smoothed to a frequency resolution of 4 Hz.

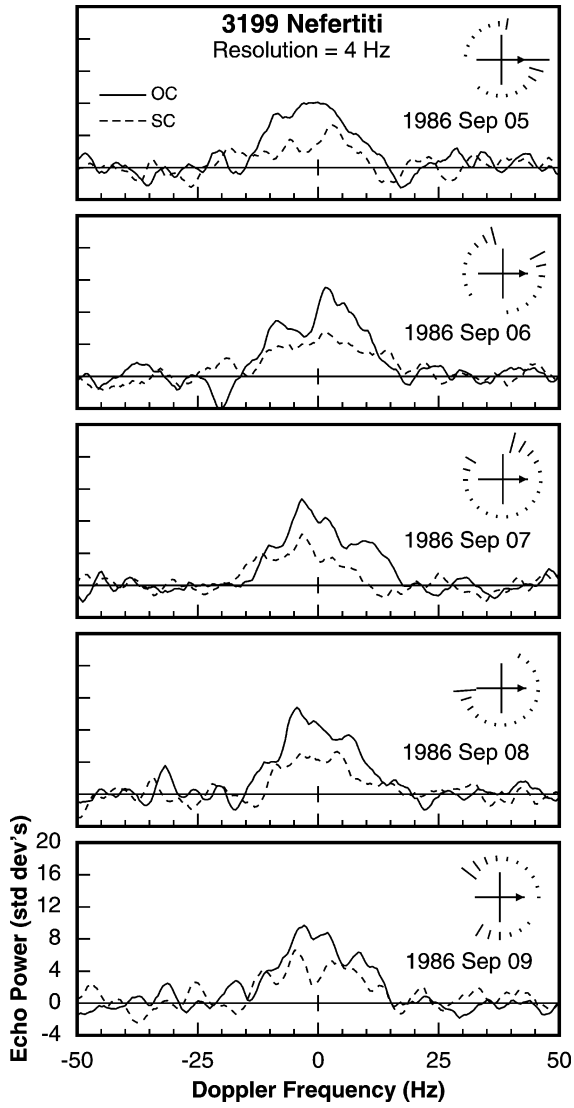

Fig. 2. Weighted sum of 3199 Nefertiti echo power spectra for each day, filtered to a frequency resolution of 4 Hz. All plots have the same vertical scale. Relative rotation phases for each sum are indicated; the length of each bar is proportional to its signal-to-noise level. The zero-phase UTC epoch is 1986 September 5 03:43:41. A vertical bar at the origin indicates ±1 standard deviation of the OC receiver noise.

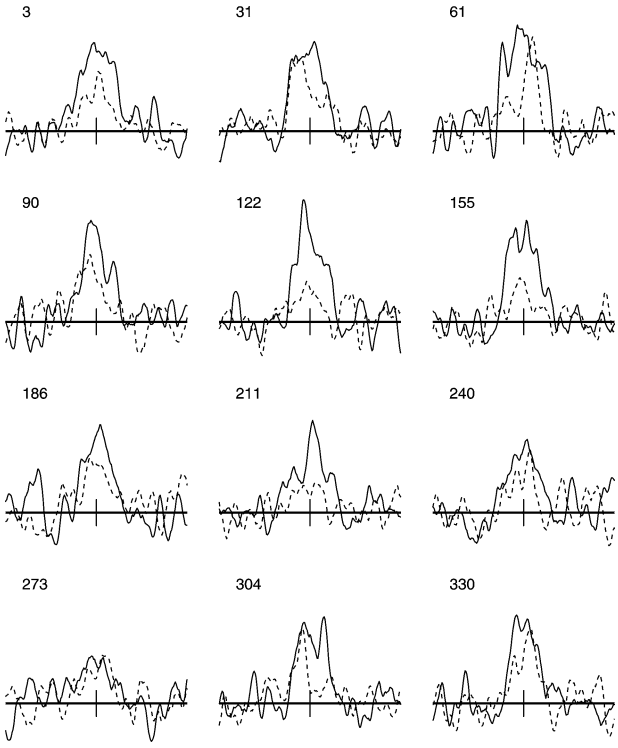

Fig. 3. Weighted summed spectra of 3199 Nefertiti blocked into 30° phase intervals and filtered to a frequency resolution of 5 Hz. Mean rotation phases (in degrees) for each sum are shown in upper left corner. Identical linear scales are used throughout the figure. Solid lines are OC and dashed lines are SC. Each horizontal axis extends from −50 Hz on the left to 50 Hz on the right. A vertical bar at 0 Hz indicates ±1 standard deviation of the OC receiver noise.

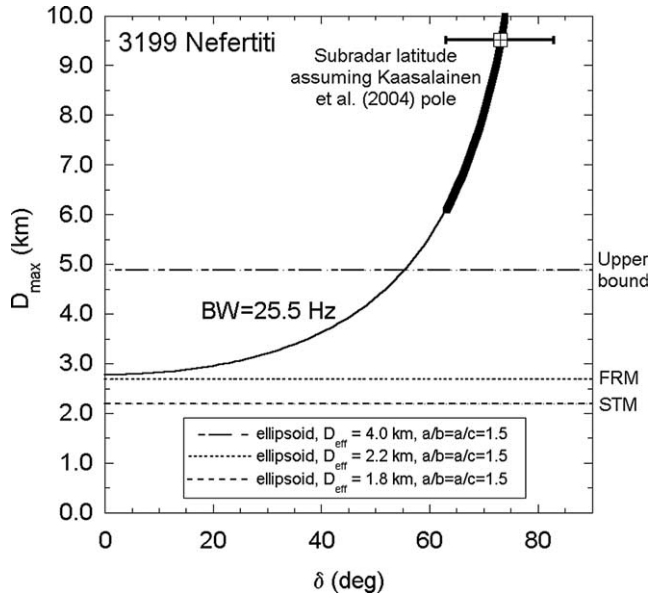

Fig. 4. Joint constraints on the size, shape, subradar latitude, and maximum equatorial diameter for 3199 Nefertiti. The thin solid line is the constraint on size due to an observed minimum bandwidth of 25.5 Hz (Eq. (3)). If Nefertiti is a sphere, then its effective diameter is represented by values of $D_{\max}$ along this line. The thin dashed lines indicate constraints on Nefertiti if it is an ellipsoid of aspect ratio $a/b = a/c = 1.5$. Three ellipsoid models with different effective diameters are shown: 1.8 km (STM), 2.2 km (FRM), and 4.0 km (upper bound based on assumed minimum optical albedo). The subradar latitude implied by the Kaasalainen et al. (2004) pole direction is indicated; the bold line indicates the range of sizes and subradar latitudes permitted by the joint constraint of their pole (including reported uncertainty) and the observed minimum radar bandwidth.

Nefertiti's OC radar cross-section is 1.2 ± 0.4 km^2. Its polarization ratio, 0.47 ± 0.04, is higher than 80% of those reported for radar-detected asteroids and suggests significant near-surface roughness (see http://echo.jpl.nasa.gov/~lance/asteroid_radar_properties.html).

Using the sum of all spectra and a two-sigma crossing threshold, we estimate Nefertiti's minimum bandwidth to be 25.5 Hz; this gives a lower bound of 2.8 km on its maximum pole-on diameter $D_{\max}$. If Nefertiti's visual albedo is at least 0.10 (i.e., consistent with an A, S, or Sq class asteroid; see Tholen and Barucci, 1989), then its absolute magnitude (Table 1) requires an effective diameter less than 4.0 km.

Figure 3 shows weighted sums of Nefertiti observations binned into 30° rotation phase intervals and filtered to an effective frequency resolution of 5.0 Hz. Two-sigma crossing thresholds range from 20 to 30 Hz, suggesting that Nefertiti's elongation is no more than 1.5 (we have ignored the bandwidth estimate at an average phase of 273° because of low SNR). This range of thresholds is consistent with Nefertiti's lightcurve amplitude (Table 1) and the elongation estimated by Kaasalainen et al. (2004). There is no evidence of spectral asymmetry.

To explore the relationships between Nefertiti's size, aspect ratio, and pole position, we plot in Fig. 4 $D_{\max}$ versus subradar latitude for ellipsoids of various sizes (D_{eff}), all of aspect ratio $a/b = a/c = 1.5$ (dashed lines). The values of D_{eff} shown correspond to reported radiometric diameters and to our upper bound. Our radar constraint on bandwidth is indicated by a solid line. If Nefertiti were a sphere, its effective diameter would be given by the values of $D_{\max}$ that fall on this line for a given subradar latitude, δ. A large square symbol indicates the subradar latitude implied by the Kaasalainen et al. (2004) pole and its associated uncertainty. The joint constraint between the radar bandwidth and Kaasalainen et al. (2004) pole direction is plotted as a bold line.

From Fig. 4, we conclude that if Nefertiti is spherical ($a/b = a/c = 1$) to moderately elongate ($a/b = a/c = 1.5$), as suggested by lightcurves and Fig. 3, then its effective diameter is *at least* 2.2 km and our subradar latitude was less than 55°. Smaller sizes require greater degrees of elongation. Our size constraint is most consistent with the radiometric diameter obtained using the FRM, suggesting that Nefertiti has a high surface thermal inertia. However, the radiometric observations of Nefertiti were made at relatively high phase angles (40°–84°, Veeder et al., 1989) where the competing effects of surface structure and thermal inertia are not well understood (Delbo et al., 2003). Our conclusion regarding Nefertiti's surface thermal inertia must therefore be considered tentative.

If Nefertiti's effective diameter lies between 2.2 and 4.0 km, then its radar albedo lies between 0.10 and 0.32. This

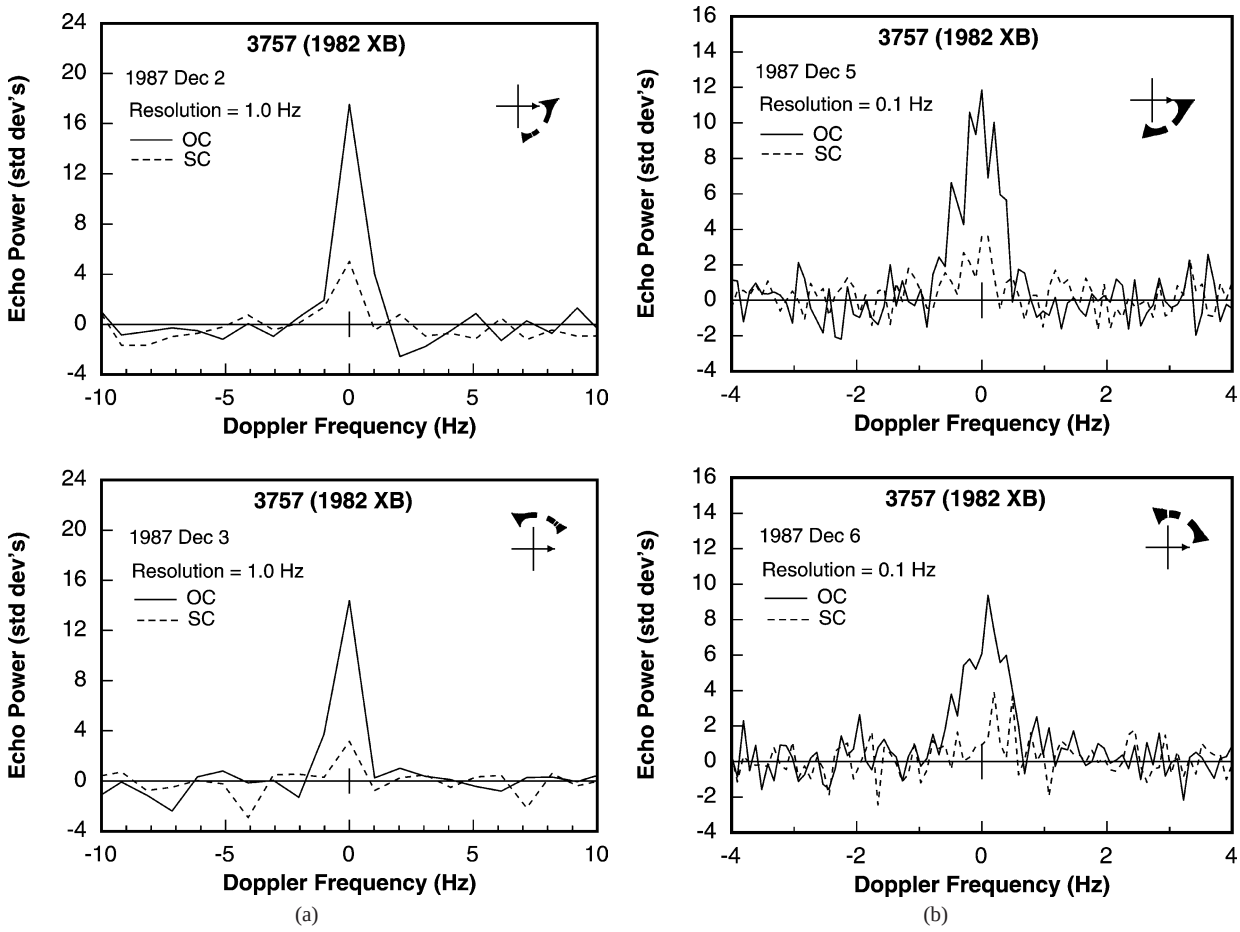

Fig. 5. Weighted sums of 1982 XB echo power spectra for each date. Relative rotation phases for each sum are indicated. The zero-phase UTC epoch is 1987 December 5 07:11:20. A vertical bar at the origin indicates ±1 standard deviation of the OC receiver noise. (a) December 2 and 3, 1.0-Hz frequency resolution. (b) December 5 and 6, 0.1-Hz frequency resolution.

range spans the middle 70% of known NEA albedos and is consistent with the average of other S-class asteroids (0.16 ± 0.02) (Ostro et al., 2002; http://echo.jpl.nasa.gov/~lance/asteroid_radar_properties.html). There are no comparative radar albedo data for any A-class asteroids.

At the midpoint of our observations, Nefertiti was located at $\lambda = 359°$, $\beta = 24°$. If we adopt the pole reported by Kaasalainen et al. (2004), then our subradar latitude was $73° \pm 10°$ (Fig. 4). For this pole direction to be consistent with our bandwidth, Nefertiti must have an equatorial diameter of at least 6 km and optical albedo no larger than 0.06. Since this seems unlikely given all the available information, we conclude that the Kaasalainen pole is incorrect.

3.3. 3757 (1982 XB)

3757 (1982 XB) is an S-class asteroid based on its reddish color and possible olivine/pyroxene absorption features (Helin et al., 1983). Diameter estimates range from 0.35 km (STM, Helin et al., 1983; Veeder et al., 1989; Harris et al., 1999) to 0.7 km (FRM, Veeder et al., 1989). Estimates of its corresponding optical albedo range from 0.09 to 0.26 (Helin et al., 1983; Veeder et al., 1989; Harris et al., 1999). 1982 XB's rotation period is $P = 9.0046 \pm 0.0013$ h (Harris et al., 1999).

1982 XB was observed at Arecibo on December 2, 3, 5, and 6 in 1987. On December 2 and 3, the frequency resolution was 1.0 Hz and we did not resolve the asteroid in frequency; a total of 70 runs with a total SNR of 23 was obtained on those dates. On December 5 and 6, the frequency resolution was increased to 0.1 Hz to resolve the asteroid; a total of 84 runs with a total SNR of 31 was obtained on those dates. Figures 5a and 5b show the single-date spectral sums. Table 3 lists the radar properties of the separately weighted sums for December 2 and 3, December 5 and 6, and their weighted average. 1982 XB's radar cross-section is $\sigma_{OC} = 0.017 \pm 0.006$ km^2, and its circular polarization ratio is $\mu_c = 0.24 \pm 0.05$, which is near the average for NEAs.

Using the weighted sum of the 0.1 Hz data and a two-sigma crossing threshold, we estimate 1982 XB's minimum bandwidth to be $B = 1.4$ Hz; combined with the 9-h rotation period, this constrains the lower bound on the maximum diameter D_{max} to be at least 0.46 km.

Figure 6 shows weighted sums of 0.1 Hz data binned by rotation phase. 1982 XB's two-sigma crossing bandwidth varies less than 20%, suggesting a small elongation and

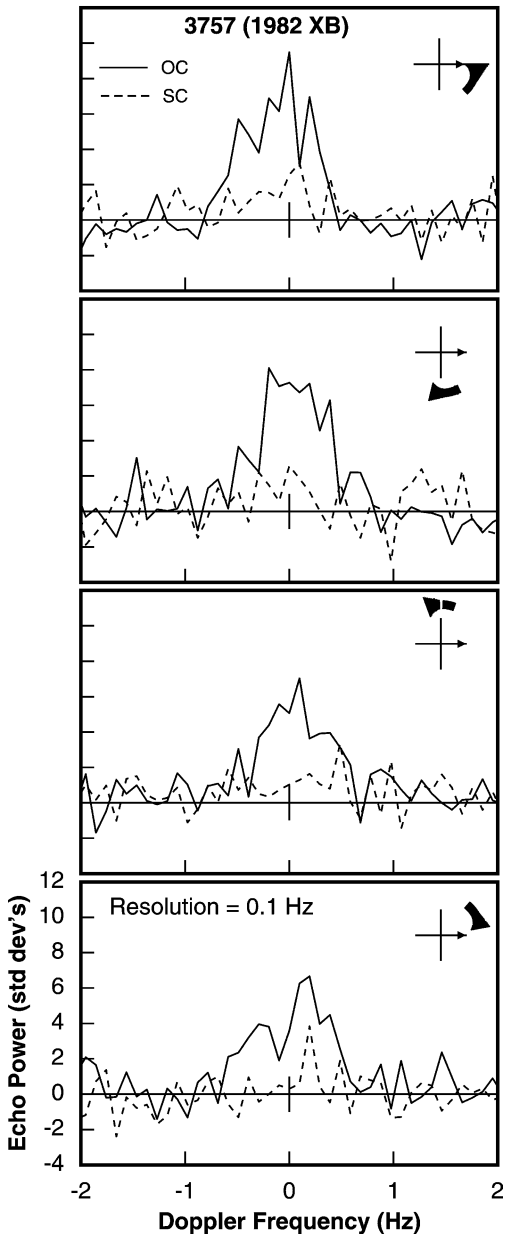

Fig. 6. Weighted sums of 1982 XB spectra from December 5 and 6, plotted at 0.1-Hz frequency resolution for rotation phase blocks about 50° wide, as indicated. A vertical bar at 0 Hz indicates ±1 standard deviation of the OC receiver noise.

consistency with its low lightcurve amplitude. If we model 1982 XB as an ellipsoid of aspect ratio $a/b = a/c = 1.2$, then its effective diameter is at least 0.4 km, consistent with all previous diameter estimates (Helin et al., 1983; Veeder et al., 1989; Harris et al., 1999).

Using 1982 XB's absolute magnitude (Table 1) and adopting $D_{\rm eff} \geqslant 0.4$ km constrain its visual albedo to be $p_v \leqslant 0.25$, which is consistent with an S classification. Adopting $p_v = 0.10$ as a lower bound on the optical albedo of S-class asteroids gives an upper bound of 0.63 km on the effective diameter, which is ∼ 10% smaller than the size estimate based on the FRM (Veeder et al., 1989). These upper

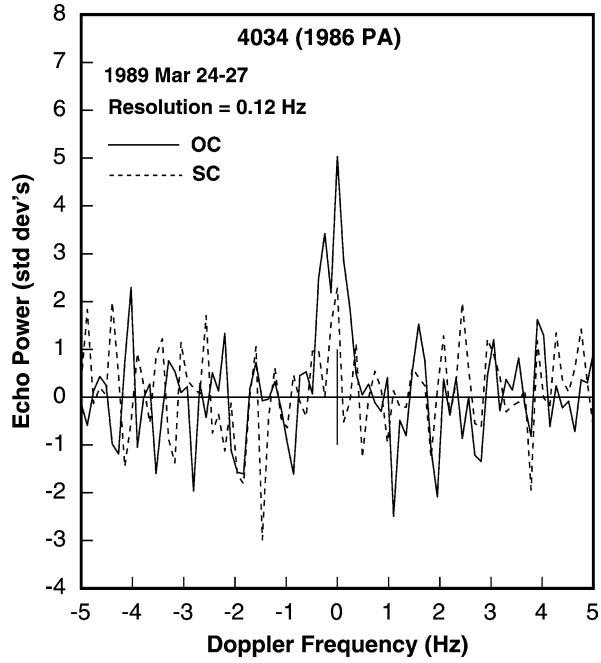

Fig. 7. Weighted sum of 1986 PA echo power spectra. The frequency resolution is 0.12 Hz. A vertical bar at the origin indicates ±1 standard deviation of the OC receiver noise.

and lower limits on size constrain the subradar latitude to be within 50° of equatorial.

Adopting $D_{\rm eff} \geqslant 0.4$ km constrains the radar albedo to be less than 0.14, which is in the lower half of NEA values (Ostro et al., 2002; http://echo.jpl.nasa.gov/~lance/asteroid_radar_properties.html). If $D_{\rm eff}$ were as large as 0.63 km, then $\hat{\sigma}_{\rm OC}$ would equal 0.05, among the lowest values observed.

3.4. 4034 (1986 PA)

4034 (1986 PA) is classified O in the Bus and Binzel (2002) system. Spectrally, the O-class asteroids are most consistent with L6 and LL6 chondrites and are therefore considered a possible source of ordinary chondrites (Binzel et al., 1993). Using infrared radiometry, Delbo et al. (2003) estimate 1986 PA's diameter to lie between 0.40 km (STM) and 0.57 km (FRM). They consider their NEATM-based size estimate of 0.42 ± 0.07 km to be the most reliable. There is considerable uncertainty in the absolute magnitude of 1986 PA (perhaps up to ±0.5 magnitudes, Delbo et al., 2003), but using the JPL Horizons (http://ssd.jpl.nasa.gov/horizons.html) absolute magnitude (Table 1) and the NEATM diameter leads to a corresponding optical albedo of $p_v = 0.58 + 0.25/-0.16$. No lightcurve data exist for this object and its rotation period is unknown.

We observed 1986 PA at Arecibo on March 24–27, 1989, acquiring a total of 58 dual-polarization runs with a frequency resolution of 0.122 Hz and a total SNR of 7. The weighted sum of all spectra is shown in Fig. 7.

We measured 1986 PA's OC radar cross-section to be $\sigma_{OC} = 0.021 \pm 0.007$ km^2. If we adopt the NEATM determined diameter of 0.42 ± 0.07 km, then we obtain a radar albedo of $\hat{\sigma}_{OC} = 0.15 + 0.14/-0.07$, which is about average for NEAs. 1986 PA's polarization ratio, $\mu_c = 0.21 \pm 0.06$, is in the lower half of NEA values. Because the echo signal strength is so low, we use the full-width-half-maximum to place a lower bound on 1986 PA's bandwidth of 0.5 Hz; when combined with a diameter of 0.42 km, this bandwidth constrains the rotation period to less than about 24 h.

4. Future observing opportunities

The next favorable opportunity for radar observation of 1986 PA is in March 2013, when SNRs of ~ 40 per day are expected at Arecibo. Lightcurve observations of 1986 PA are needed to estimate its rotation period. The next photometric opportunities occur in August of 2009 and 2010 when the asteroid's apparent visual magnitude will be 17.7 and 17.4, respectively, and within the reach of a meter-class telescope (see http://echo.jpl.nasa.gov/~lance/radar.nea.periods.html for a list of upcoming apparitions for radar targets). The next opportunities for radar observations of Quetzalcoatl, Nefertiti, and 1982 XB occur in February 2114, September 2065, and January 2070, respectively.

Acknowledgments

We thank A.W. Harris (DLR) and an anonymous reviewer for their reviews. We thank the staff at the Arecibo Observatory for technical assistance with the observations. Part of this research was conducted at the Jet Propulsion Laboratory, California Institute of Technology, under contract with the National Aeronautics and Space Administration. Work at the Center for Astrophysics was supported in part by the National Aeronautics and Space Administration. The Arecibo Observatory is part of the National Astronomy and Ionosphere Center, which is operated by Cornell University under a cooperative agreement with the National Science Foundation and with support from the National Aeronautics and Space Administration.

References

Binzel, R.P., Tholen, D.J., 1983. The rotation, color, phase coefficient, and diameter of 1915 Quetzalcoatl. Icarus 55, 495–497.

Binzel, R.P., Xu, S., Bus, S.J., Skrutskie, M.F., Meyer, M.R., Knezek, P., Barker, E.S., 1993. Discovery of a main-belt asteroid resembling ordinary chondrite meteorites. Science 262, 1541–1543.

Bus, S.J., Binzel, R.P., 2002. Phase II of the small main-belt asteroid spectroscopic survey: a feature-based taxonomy. Icarus 158, 146–177.

Binzel, R.P., Birlan, M., Bus, S.J., Harris, A.W., Rivkin, A.S., Fornasier, S., 2004. Spectral observations for near-Earth objects including potential target 4660 Nereus: results from Meudon remote observations at the NASA Infrared Telescope Facility (IRTF). Planet. Space Sci. 52, 291–296.

Cruikshank, D.P., Hartmann, W.K., Tholen, D., Bell, J., 1985. An olivine-rich Earth crossing asteroid: source of pallasites? In: Proc. Lunar Planet. Sci. Conf. 16th, p. 160. Abstract.

Delbo, M., Harris, A.W., Binzel, R.P., Pravec, P., Davies, J.K., 2003. Keck observations of near-Earth asteroids in the thermal infrared. Icarus 166, 116–130.

Fowler, J.W., Chillemi, J.R., 1992. IRAS asteroid data processing. In: Tedesco, E.F. (Ed.), IRAS Minor Planet Survey, Tech. Rpt. PL-TR-92-2049. Phillips Laboratory, Hanscom Air Force Base, Massachusetts, pp. 17–43.

Harris, A.W., 1998. A thermal model for near-Earth asteroids. Icarus 131, 291–301.

Harris, A.W., Lagerros, J.S.V., 2002. Asteroids in the thermal infrared. In: Bottke Jr., W.F., Cellino, A., Paolicchi, P., Binzel, R.P. (Eds.), Asteroids III. Univ. of Arizona Press, Tucson, pp. 205–218.

Harris, A.W., Young, J.W., Bowell, E., Tholen, D., 1999. Asteroid lightcurve observations from 1981 to 1983. Icarus 142, 173–201.

Helin, E.F., Harris, A.W., Young, J.W., Tedesco, E.F., Lebofsky, L.A., Tholen, D., Binzel, R.P., Hulkower, N.D., 1983. A new Earth-approaching asteroid: 1982 XB. In: Proc. Lunar Planet. Sci. Conf. 14th, pp. 297–298. Abstract.

Kaasalainen, M., Pravec, P., Krugly, Y.J., Sarounova, L., Torppa, J., Virtanen, J., Kaasalainen, S., Erikson, A., Nathues, A., Durech, J., Wolf, M., Lagerros, J.S.V., Lindgren, M., Lagerkvist, C.I., Koff, R., Davies, J., Mann, R., Kusnirak, P., Gaftonyuk, N.M., Shevchenko, V.G., Chiorny, V.G., Belskaya, I.N., 2004. Photometry and models of eight near-Earth asteroids. Icarus 167, 178–196.

Lebofsky, L.A., Veeder, G.J., Lebofsky, M.J., Matson, D.L., 1978. Visual and radiometric photometry of 1580 Betulia. Icarus 35, 336–343.

Lebofsky, L.A., Spencer, J.R., 1989. Radiometry and thermal modeling of asteroids. In: Binzel, R.P., Gehrels, T., Matthews, M.S. (Eds.), Asteroids II. Univ. of Arizona Press, Tucson, pp. 128–147.

Magri, C., Ostro, S.J., Rosema, K.D., Thomas, M.L., Mitchell, D.L., Campbell, D.B., Chandler, J.F., Shapiro, I.I., Giorgini, J.D., Yeomans, D.K., 1999. Main-belt asteroids: results of Arecibo and Goldstone observations of 37 objects during 1980–1995. Icarus 140, 379–407.

Mahapatra, P.R., Ostro, S.J., Benner, L.A.M., Rosema, K.D., Jurgens, R.F., Winkler, R., Rose, R., Giorgini, J.D., Yeomans, D.K., Slade, M.A., 1999. Recent radar observations of Asteroid 1566 Icarus. Planet. Space Sci. 47, 987–995.

Margot, J.-L., Brown, M.E., 2003. A low-density M-type asteroid in the main belt. Science 300, 1939–1942.

Mitchell, D.L., Ostro, S.J., Rosema, K.D., Hudson, R.S., Campbell, D.B., Chandler, J.F., Shapiro, I.I., 1995. Radar observations of Asteroids 7 Iris, 9 Metis, 12 Victoria, 216 Kleopatra, and 654 Zelinda. Icarus 118, 105–131.

Mitchell, D.L., Ostro, S.J., Hudson, R.S., Rosema, K.D., Campbell, D.B., Velez, R., Chandler, J.F., Shapiro, I.I., Giorgini, J.D., Yeomans, D.K., 1996. Radar observations of Asteroids 1 Ceres, 2 Pallas, and 4 Vesta. Icarus 124, 113–133.

Ostro, S.J., Campbell, D.B., Chandler, J.F., Shapiro, I.I., Hine, A.A., Velez, R., Jurgens, R.F., Rosema, K.D., Winkler, R., Yeomans, D.K., 1991a. Asteroid radar astrometry. Astron. J. 102, 1490–1502.

Ostro, S.J., Campbell, D.B., Chandler, J.F., Hine, A.A., Hudson, R.S., Rosema, K.D., Shapiro, I.I., 1991b. Asteroid 1986 DA: radar evidence for a metallic composition. Science 252, 1399–1404.

Ostro, S.J., Hudson, R.S., Nolan, M.C., Margot, J.-L., Scheeres, D.J., Campbell, D.B., Magri, C., Giorgini, J.D., Yeomans, D.K., 2000. Radar observations of Asteroid 216 Kleopatra. Science 288, 836–839.

Ostro, S.J., Hudson, R.S., Benner, L.A.M., Giorgini, J.D., Magri, C., Margot, J.L., Nolan, M.C., 2002. Asteroid radar astronomy. In: Bottke Jr., W.F., Cellino, A., Paolicchi, P., Binzel, R.P. (Eds.), Asteroids III. Univ. of Arizona Press, Tucson, pp. 255–271.

Pravec, P., Wolf, M., Sarounova, L., Mottola, S., Erikson, A., Hahn, G., Harris, A.W., Harris, A.W., Young, J.W., 1997. The near-Earth objects follow-up program II. Results for 8 asteroids from 1982 to 1995. Icarus 130, 275–286.

Rabinowitz, D.L., Shoemaker, E.M., Bowell, E., Muinonen, K., 1994. The population of Earth-crossing asteroids. In: Gehrels, T. (Ed.), Hazards due to Asteroids and Comets. Univ. of Arizona Press, Tucson, pp. 285–312.

Tholen, D., 1989. Asteroid taxonomic classifications. In: Binzel, R.P., Gehrels, T., Matthews, M.S. (Eds.), Asteroids II. Univ. of Arizona Press, Tucson, pp. 1139–1150.

Tholen, D., Barucci, M.A., 1989. Asteroid taxonomy. In: Binzel, R.P., Gehrels, T., Matthews, M.S. (Eds.), Asteroids II. Univ. of Arizona Press, Tucson, pp. 298–315.

Veeder, G.D., Hanner, M.S., Matson, D.L., Tedesco, E.F., Lebofsky, L.A., Tokunaga, A.T., 1989. Radiometry of near-Earth asteroids. Astron. J. 97, 1211–1219.